Article

Not peer-reviewed version

Moderate Overweight of Male Rats Chronically Fed with a Hyperlipidic Diet Developed Early Silent Ang-(3–4)-Sensitive Myocardial Molecular Lesions and Preserved Echographic Parameters

Thuany Crisóstomo , Rafael Luzes , Matheus Leonardo Lima Gonçalves , Marco Antônio Estrela Pardal , Humberto Muzi-Filho , Glória Costa-Sarmento , Debora B. Mello , Adalberto Vieyra *

Posted Date: 15 July 2024

doi: 10.20944/preprints202407.1120.v1

Keywords: overweight/obesity; hypertension; hyperlipidic diets; pro-inflammatory cytokines; cardiometabolic diseases; renin-angiotensin-aldosterone system; Ang-(3–4); cardiac ion-transporting ATPases; cardiac echocardiography

Article

Moderate Overweight of Male Rats Chronically Fed with a Hyperlipidic Diet Developed Early Silent Ang-(3–4)-Sensitive Myocardial Molecular Lesions and Preserved Echographic Parameters

Thuany Crisóstomo [1], Rafael Luzes [2], Matheus Leonardo Lima Gonçalves [3], Marco Antônio Estrela Pardal [4], Humberto Muzi-Filho [4], Glória Costa-Sarmento [4], Debora B. Mello [5] and Adalberto Vieyra [2,4,5,*]

[1] Leopoldo de Meis Institute of Medical Biochemistry, Federal University of Rio de Janeiro, 21941-902 Rio de Janeiro, Brazil; thuany.crisostomo@bioqmed.ufrj.br
[2] Graduate Program in Translational Biomedicine/BIOTRANS, Grande Rio University/UNIGRANRIO, 25071-202 Duque de Caxias, Brazil; rafael.luzes@abeugraduacao.com.br (R.L.); avieyra@biof.ufrj.br (A.V.)
[3] Grande Rio University/UNIGRANRIO, 25071-202 Duque de Caxias, Brazil; matheusunigranrio@outlook.com (M.L.L.G)
[4] Carlos Chagas Filho Institute of Biophysics, Federal University of Rio de Janeiro, 21941-902 Rio de Janeiro, Brazil; marco.pardal20@gmail.com (M.A.E.P.); humbertomuzi@biof.ufrj.br (H.M-F.); sarmento@biof.ufrj.br (G.C-S.); avieyra@biof.ufrj.br (A.V.)
[5] National Center for Structural Biology and Bioimaging/CENABIO, Federal University of Rio de Janeiro, 21941-902 Rio de Janeiro, Brazil; debmello@cenabio.ufrj.br; (D.B.M.); avieyra@biof.ufrj.br (A.V.)
* Correspondence: avieyra@biof.ufrj.br

Abstract: Overweight/obesity and cardiovascular diseases are associated with high rates of mobility and mortality. We investigated inflammatory lesions and ionic transporters in the left ventricle of male rats chronically fed a high-fat diet (HL). They developed moderate overweight with early expansion of visceral adiposity. The inflammatory markers interleukin-6 (IL-6) and tumor necrosis factor-alpha (TNF-α), Na^+-transporting ATPases, sarco-endoplasmic reticulum Ca^{2+}-ATPase (SERCA2a), and the abundance of Angiotensin II receptors were studied together with lipid and glycemic profiles, and the left ventricle echocardiographic parameters fractional shortening (FS) and ejection fraction (EF). HL rats doubled IL-6 and TNF-α, which returned to normal levels when signaling coupled to Angiotensin II type 2 receptors (AT_2R) was supraregulated by Ang-(3–4) administration. The decreased glucose tolerance was accompanied by significantly reduced plasma triglycerides due to intense hepatic steatosis (Crisóstomo et al. *Metabolism Open*. 2022, 14, 100176). AT_2R (and AT_1R) abundance did not change. $(Na^+ + K^+)$ATPase and ouabain-resistant Na^+-ATPase were downregulated and upregulated, respectively, normalized with Ang-(3–4). SERCA2a lost its most critical regulatory property, inhibition by excess substrate. The ultrasound showed no changes in FS and EF. We conclude that very moderate overweight can cause silent initial molecular tissue damage in heart, which can evolve to cause systolic dysfunction.

Keywords: overweight/obesity; hypertension; hyperlipidic diets; pro-inflammatory cytokines; cardiometabolic diseases; renin-angiotensin-aldosterone system; Ang-(3–4); cardiac ion-transporting ATPases; cardiac echocardiography

1. Introduction

The combination of overweight and obesity is currently considered a true pandemic that, together with malnutrition and climate changes, is part of the first significant syndemic of the 21st century [1]. Recent data from the World Health Organization [2] indicate that global adult obesity has more than doubled since 1990 and that among adolescents has quadrupled. In 2022 [3], out of a total world population of 8 billion, 2.5 billion adults over 18 were overweight; of these, 890 million

 doi:10.20944/preprints202407.1120.v1

were obese. Data from 2018 [4] show that mortality associated with overweight/obesity is high: around 50/1,000 adults per year in the case of overweight and around 70/1,000 adults per year in the case of obesity. It is important to emphasize that there is a marked increase in the incidence of overweight and obesity in children, adolescents, and young adults, which evolves into the same condition – generally associated with severe comorbidities – in adulthood [5,6].

Overweight and obesity result from a long period of positive energy balance and the inability to control food (and energy) intake and expenditure [7]. The composition of diets, especially "Western" ones [8], rich in fats and sugars, has been considered for more than two decades as one of the most critical factors in the development of overweight and obesity [9,10]. Diets that are often accompanied by a high salt content [11].

Among the processes and mechanisms that lead to severe comorbidities, including hypertension, coronary disease and metabolic syndrome (dyslipidemia, type 2 diabetes), the renin aldosterone system (RAAS) plays a significant role. It contributes to insulin resistance and stimulates inflammatory processes [8]. Research from our laboratory [12] has shown that overweight rats have a hyperactivated renal tissue RAAS with upregulation of Na^+ transporting ATPases, significant interstitial fibrosis as a result of an early inflammatory process and expansion of visceral fat.

The present study aimed to investigate cardiometabolic changes in young [13] and moderately overweight hypertensive male rats chronically feeding with a high-fat and high-caloric diet [14]. Looking for possible inflammatory cellular and molecular changes and ionic transporters in the left ventricle, potentially associated with hyperactivity of the local cardiac RAAS [15] arm coupled to type 1 Ang II receptors. Furthermore, we intended to investigate whether these changes are reflected in the echocardiographic structure and function of the heart, as well as the result of activation of the RAAS arm coupled to type 2 Ang II receptors by Ang-(3–4) [16], the antagonist of the effects of Ang II in different physiological and pathological conditions [17,18].

It is concluded that moderate overweight resulting from the chronic intake of a high-fat diet that mimics the so-called "Western diets" [8] causes early cardiometabolic changes and in the active transport of Na^+ and Ca^{2+} in the myocardial tissue of young hypertensive rats. These changes coexist with a shortening fraction and an ejection fraction still preserved.

2. Results

2.1. Development of Moderate Overweight in Rats that Received the High-fat Diet

Figure 1 shows that rats weighing an average of 259 g at 58 days of age fed the HL diet developed moderate – but significant – overweight 106 days later compared to CTR rats. This last group, fed with a diet prepared following the recommendations of AI-93 [19] containing 385 kcal/100 g of dry food with 9 % of calories coming from lipids, reached an average body mass of 458 ± 15 g. Meanwhile, the group exposed to the hypercaloric and high-fat HL diet (574 kcal/100 g of dry food with 70 % of calories coming from lipids) reached a body mass of 506 ± 16 g, i.e. 10 % greater. These values are close to the asymptotic value of the previously described growth curves [12], that is, the upper limits of growth.

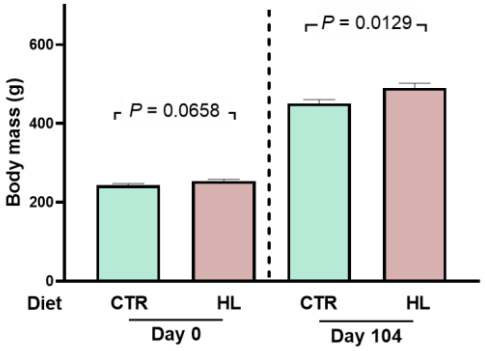

 doi:10.20944/preprints202407.1120.v1

Figure 1. The administration of the high lipid (HL) diet during 104 days from day 58 of life leads to a small but significant overweight of male rats. Left: body mass at the beginning of different dietary exposures (zero time). Right: body mass 104 days later. Diets and days of exposure to the different diets are indicated on the abscissae; n = 30 (CTR rats) and n = 26 (HL rats). Bars show mean ± SEM. Differences on the same day were assessed using unpaired Student's *t*-test; *p* values are indicated within the panel.

It is clear that the decrease in food and energy intake in HL rats, without influence on CTR rats [12], does not explain the small changes in body mass observed in Figure 2, which could even accompany changes in other parameters on the influence of Ang-(3–4) was tested. Therefore, water intake, urinary volume, and water balance were analyzed 24 h after administration of Ang-(3–4).

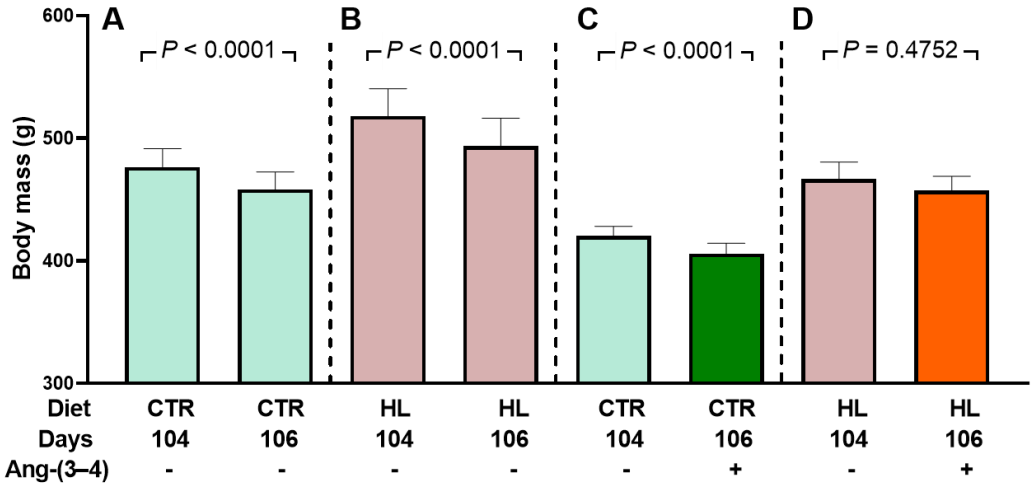

Figure 2. Evolution of body mass when the rats are housed in metabolic cages: effect of Ang-(3–4) administration (4 doses on days 104 and 105). Diets, days of exposure to the different diets at the end of the study, and administration or not of Ang-(3–4) are indicated on the abscissae. CTR (n = 30) and HL (n = 26) rats were divided into two subgroups. One of them was to follow body mass evolution without Ang-(3–4) treatment between days 104 and 106 (n = 17 and 12 for CTR and HL, respectively) (**A** and **B**). The other group was to follow body mass evolution after Ang-(3–4) administration (n = 13 and 14 for CTR and HL, respectively) (**C** and **D**). Bars show mean ± SEM. Differences between days 104 and 106 in each subgroup were assessed using paired Student's *t*-test; *p* values are indicated within the panels.

Figure 3 shows that the administration of Ang-(3–4) causes an increase in water intake in CTR rats (**A**), which is accompanied by a proportionally similar increase in urinary volume over the same period (**B**). These changes in parallel result in an unmodified water balance in CTR rats receiving Ang-(3–4)(**C**). In the case of the treated HL group, whose liquid intake is lower (**A**), urinary volume (**B**) had values that also resulted in an unmodified water balance after administration of Ang-(3–4) (**C**). The comparison of studies on food and caloric intake [12] and water balance (the present work) allows us to conclude that housing rodents in metabolic cages alone or accompanied by the brief administration of Ang-(3–4), has an intrinsic variability whose causes remain open, as recently demonstrated [20]. That is why these still-ununderstood modifications must be considered when analyzing materials collected in these cages or Ang-(3–4)-induced modifications in other functions, processes, or organs. This point will be discussed again later.

 doi:10.20944/preprints202407.1120.v1

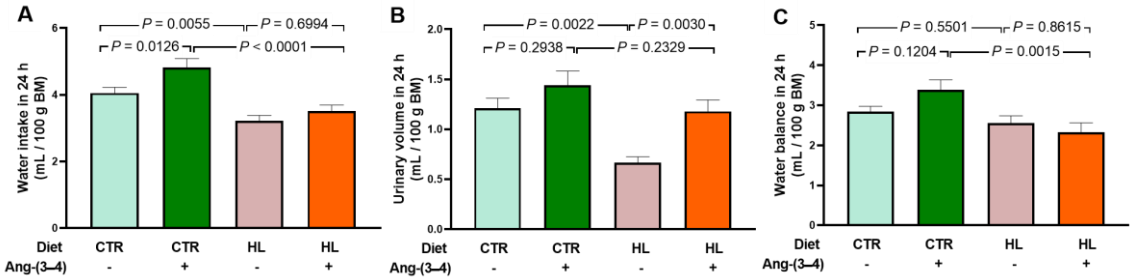

Figure 3. Water intake (**A**), urinary volume (**B**), and water balance (**C**) in 24 h measured on day 106. After administering or not 4 doses of Ang-(3–4) on days 104 and 105, measurements were carried out. Diets and administration or not of Ang-(3–4) are indicated on the abscissae; n = 10–16. Bars show mean ± SEM. Differences were assessed using two-way ANOVA followed by Bonferroni's test; *p* values are indicated within the panels.

2.2. Biomarkers of Metabolic Alterations and Inflammatory Processes in HL Overweight Rats

Just over a decade ago, the deposition of visceral fat in the perirenal subcompartment called the renal sinus was associated with severe forms of hypertension [21]. Moreover, epididymal fat is considered a marker of visceral fat [22], in which genes are found differentially expressed in obese rats due to an alimentation with a diet rich in lipids 23]. In Figure 4, it can be seen that both epididymal fat (**A**) and perirenal fat (**B**) increased by approximately 50 % in HL rats that developed moderate overweight (~10 %) after ingesting a diet rich in lipids for 104 days. The administration of 4 doses of Ang (3–4) significantly modify visceral fat levels around the 2 organs within 48 h only in HL rats.

Obesity is frequently associated with inflammation of fat tissue, especially visceral fat, and the release of pro-inflammatory cytokines [24–26]. The questions formulated based on the results obtained with visceral fat (Figure 4) were: (i) would there be an increase in pro-inflammatory cytokines in left ventricular microsomes? (ii) would there be Ang-(3-4) effects? The cytokines IL-6 and TNF-α were chosen because the former is known for establishing insulin resistance associated with obesity [24]. TNF-α because of its role in the genesis of fibrosis, previously observed [27]. Regarding IL-6, Figure 5 shows that its levels in left ventricular microsomes become ~40 % higher in HL rats when compared to CTR animals (**A** and **C**). These figures also show the opposite effects of Ang-(3-4): return to CTR values in the HL rats and increase to those found in HL rats not treated with Ang-(3–4). Observations that allow us to preliminarily conclude that the effects of Ang-(3–4) – as in other processes [17,18] – depend on states of activation/inhibition of pathways with different targets and functions. This point will be analyzed again in the Discussion section. When analyzing the TNF-α profile in the same microsomes, an increase of ~40 % in HL rats is also found, with a return to CTR values in the HL + Ang-(3-4) group and no influence in the CTR + Ang-(3-4) group (**B** and **D**).

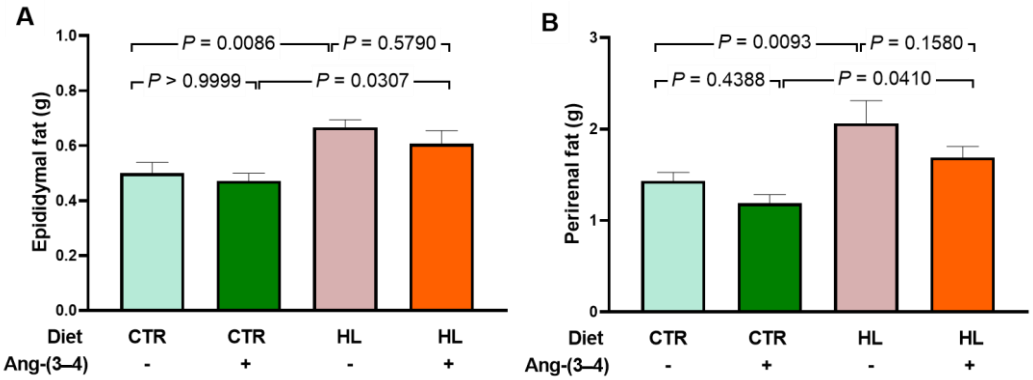

Figure 4. Augmented visceral fat in HL rats. After administering or not 4 doses of Ang-(3–4) on days 104 and 105, measurements were carried out on day 106. Diets and administration or not of Ang-(3–

 doi:10.20944/preprints202407.1120.v1

4) are indicated on the abscissae. (**A**) Epididymal fat. (**B**) Perirenal fat. Bars show mean ± SEM (n = 11–17). Differences were assessed using two-way ANOVA followed by Bonferroni's test; *p* values are indicated within the panels.

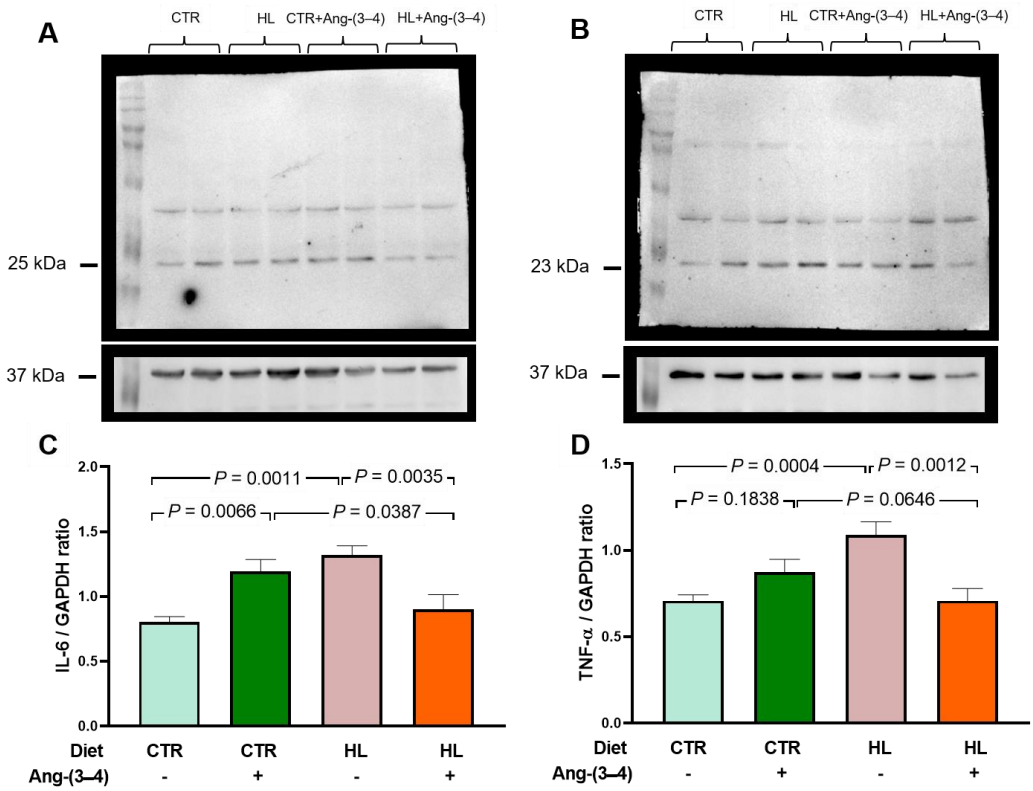

Figure 5. Increased proinflammatory cytokines in microsomes of left ventricle cardiomyocytes from HL rats: recovery of control levels after Ang-(3–4) administration. (**A**) Representative Western blottings of IL-6 (25 kDa). (**B**) Representative Western blottings of TNF-α (23 kDa). Upper lanes, cytokines; bottom lanes, loading control, GAPDH (37 kDa). (**C**) Quantification of IL-6 levels. (**D**) Quantification of TNF-α levels. After administering 4 doses of Ang-(3–4) on days 104 and 105, measurements were carried out on day 106. Diets and administration or not of Ang-(3–4) are indicated above the blottings (**A** and **B**) and on the abscissae (**C** and **D**). Bars show mean ± SEM (n = 6 different preparations of cardiac microsomes that were the same for measuring both cytokines). Differences were assessed using two-way ANOVA followed by Bonferroni's test; *p* values are indicated within the panels.

2.3. Atypical Metabolic Syndrome in HL Overweight Rats

The results described in this section present evidence that overweight (Figures 1 and 2) and hypertension in HL rats [12,27] are accompanied by an atypical metabolic syndrome. Already at the time of the onset of hypertension, i.e., 70 days of exposure to the high-fat diet [12], HL rats present a metabolic syndrome with a peculiar characteristic. Figure 6 shows that, although total cholesterol is similar in CTR and HL rats (**A**), and they show a marked decrease of 50 % in high-density lipoproteins (**B**) and a mirrored increase in low-density lipoproteins (**C**), total triglycerides are also reduced by just over 50 % (**D**).

Changes in glucose metabolism also characterize metabolic syndrome in HL rats. They present a moderate but significant increase in fasting blood glucose (Figure 7A) and glucose intolerance (Figure 7B,C), which is already predicted by changes in the lipid profile.

Preprints.org (www.preprints.org) | NOT PEER-REVIEWED | Posted: 15 July 2024 doi:10.20944/preprints202407.1120.v1

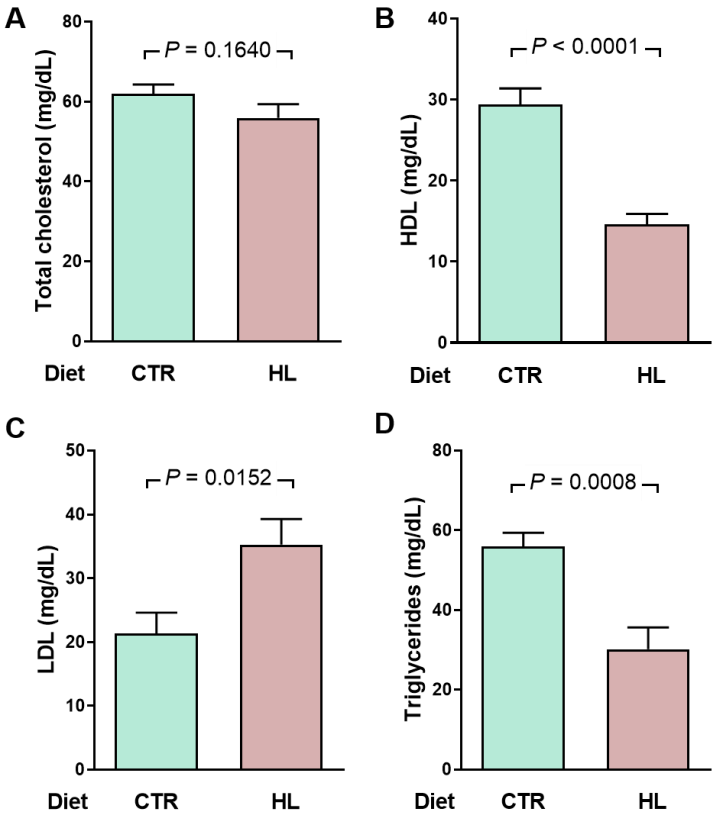

Figure 6. An early atypical lipidogram in overweight rats was encountered after 70 days of exposure to the HL diet (128 days of life). (**A**) total cholesterol (TC), (**B**) high-density lipoproteins (HDL), (**C**) low-density lipoproteins (LDL), and (**D**) Triglycerides (TG) were measured in the same plasma samples (n = 10 for CTR and HL groups). LDL cholesterol was estimated using the empirical formula LDL = TC - HDL - TG/5 [28]. Diets are indicated on the abscissae. Bars show mean ± SEM. Differences were assessed using unpaired Student's *t*-test; *p* values are indicated within the panels.

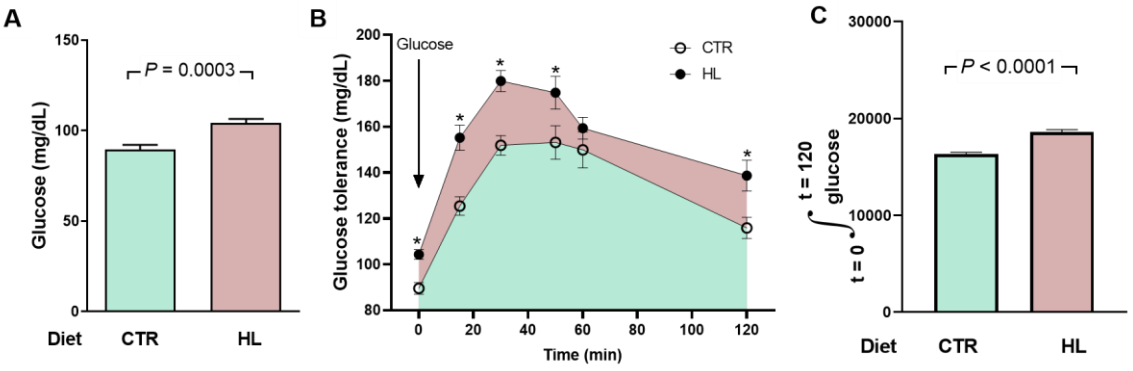

Figure 7. Moderate hyperglycemia and impaired glucose tolerance in HL rats. (**A**) After 95 days on the different diets (153 days of life), the rats (n = 10 for CTR and HL) were fasted for 12 h for a first determination of blood glucose (groups indicated on the abscissa). Bars correspond to mean ± SEM. The difference was analyzed using unpaired Student's *t*-test (*p* value shown within panel). (**B**) After blood collection to determine fasting blood glucose, the rats received glucose by gavage (arrow), and plasma concentrations were measured at the times indicated on the abscissa. The points correspond to mean ± SEM. Statistical comparison between means at each time point was performed using the unpaired Student's *t*-test. * $p < 0.05$ ranging between 0.0003 and 0.0497. The pink area shows the extra

 doi:10.20944/preprints202407.1120.v1

area under the curve in HL rats. (**C**) Quantifying the area under the glucose tolerance curves corresponding to CTR and HL rats. Bars represent mean ± SEM. The difference was investigated using the unpaired Student's *t*-test (*p* value indicated within the panel).

2.4. Unmodified Angiotensin II Receptors in Left Ventricle Microsomes from HL Rats

Figure 8A,C shows that the abundance of AT_1R in left ventricular microsomes is not modified in HL rats compared to CTR rats. Moreover, Ang-(3–4) had no effect either. In Figure 8B,D, it is observed that there were no changes in the abundance of AT_2R. These results contrast with what is found in renal proximal tubules. In the latter, there is a marked upregulation of AT_1R suppressed by Ang-(3–4), concomitantly with the downregulation of AT_2R. This contrast suggests that the primary lesion of the recently described hepatocardiorenal syndrome in overweight rats [27] would occur in the kidneys.

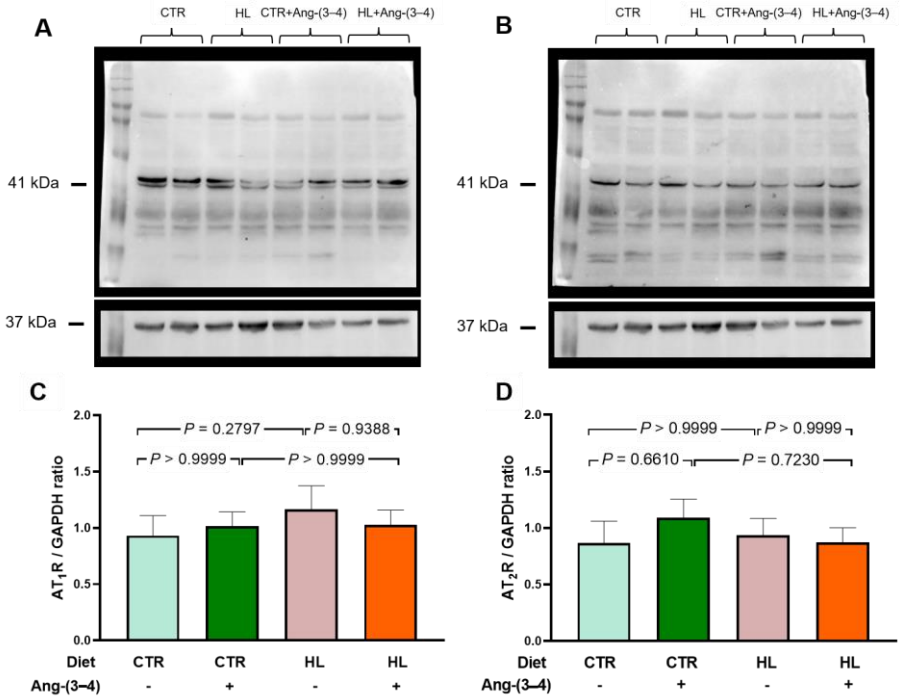

Figure 8. The abundance of Ang II receptors in microsomes of left ventricle cardiomyocytes in overweight rats remains unmodified at day 106. AT_1R (**A** and **C**) protein levels and AT_2R (**B** and **D**) were measured after 106 days of exposure to the different diets. Ang-(3–4) (4 doses) was administrated during days 104 and 105. Combinations of diets and treatment or not with Ang-(3–4) are indicated above the blottings in **A** and **B**, where 41 and 37 kDa correspond to the molecular masses of Ang II receptors and the loading control GAPDH, respectively. The combinations are also indicated on the abscissae of the receptor's quantification panels (**C** and **D**), which show mean ± SEM; n = 7–8. Differences were assessed using two-way ANOVA followed by Bonferroni's test; *p* values are indicated within the panels.

2.5. Overweight Rats Present Alterations in the Active Transport of Na^+ and Ca^{2+} in Left Ventricle that Are Reverted by Ang-(3–4)

The results below show the modifications of left ventricular ATPases, primary active transporters of Na^+ in the plasma membrane, and Ca^{2+} across the sarco-endoplasmic reticulum membrane in HL rats. The first participates in events related to electrical activity, and the second plays a central role in the contractile process. Figure 9A shows that rats that received the high-fat diet showed a marked decrease in $(Na^+ + K^+)$ATPase activity, which was recovered in animals treated with Ang-(3–4). Administration of the peptide did not influence the pump from CTR rats.

Preprints.org (www.preprints.org) | NOT PEER-REVIEWED | Posted: 15 July 2024 doi:10.20944/preprints202407.1120.v1

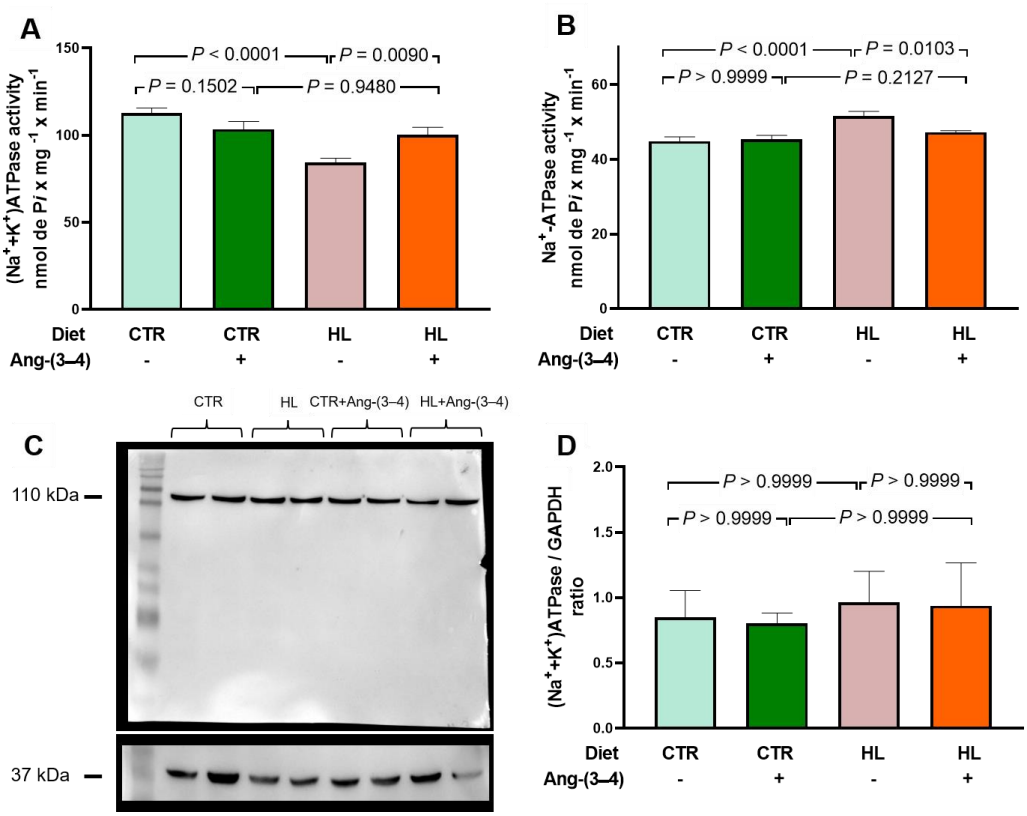

Figure 9. Opposite profiles of Na^+-transporting ATPases activities in microsomes of left ventricle cardiomyocytes from overweight rats. Combinations of diets and treatment or not with Ang-(3–4) are indicated on the abscissae and above the representative Western blotting. (**A**) Ouabain-sensitive (Na^++K^+)ATPase activity. (**B**) Ouabain-resistant, furosemide-sensitive Na^+-ATPase activity. Bars show mean ± SEM; n = 8 in all cases, using different microsome preparations. (**C**) Representative Western blotting of ouabain-sensitive (Na^++K^+)ATPase; 110 kDa and 37 kDa correspond to the molecular masses of the α-catalytic subunit of (Na^++K^+)ATPase and GAPDH, respectively. (**D**) Quantification of the immunodetections of ouabain-sensitive (Na^++K^+)ATPase corrected by the loading control. Bars show mean ± SEM; n = 4 microsome preparations. In **A**, **B**, and **D**, the differences were assessed using two-way ANOVA followed by Bonferroni's test; *p* values are indicated within the panels.

The analysis of the SERCA2a activity results (Figure 10) aimed to investigate which function best described the dependence on ATP concentration ([ATP]) because of the role of the nucleotide in excitation/contraction coupling and the importance of changes in mitochondrial energetics in the genesis of heart failure [29]. For this, two simulations were carried out using the values of the velocities averages for each [ATP] using two functions: a Michaelis Menten function (Equation 1) and another that considers the existence of inhibition due to excess substrate (Equation 2), one of the most common deviations from Michaelian kinetics of physiological significance [30]. In this second case, an activation phase is followed by another of progressive inhibition, complete or incomplete. The velocity equations used were as follows.

$$V = (V_{max} \times [ATP])/(K_{m\,ATP} + [ATP]) \quad (1)$$

$$V = (V_{max} \times [ATP])/\{(K_{m\,ATP} + [ATP]) \times (1 + [ATP]/K_{i\,ATP})\} \quad (2)$$

Figure 10**A** shows the curves that best fit the respective means: in black CTR, in red HL, in blue CTR + Ang-(3-4), and in green HL + Ang-(3-4). The Michaelian equation 1 was the one that best adjusted to the mean points of the HL group and equation 2 to the remaining 3 groups. Five curves were generated for each group, one for each experiment, and from the values obtained, V_{max}, $K_{m\,ATP}$, and $K_{i\,ATP}$ were calculated (Figure 10**B**, **C**, and **D**, respectively). About V_{max}, Km ATP, and $K_{i\,ATP}$, no significant differences were found between the CTR and HL groups, nor when analyzing activities

 doi:10.20944/preprints202407.1120.v1

with [ATP] = 5 mM (t = 0.66; p = 0.5269), a concentration close to that of cardiomyocytes in both contraction and relaxation [31]. The differences in V between these 2 groups become significant at lower ATP concentrations, such as 1 mM (t = 5.65, p = 0.0005). Ang-(3 – a 4) stimulated SERCA2a activity, increasing V_{max} and $K_{m\ ATP}$ in both the CTR and HL groups, decreasing $K_{i\ ATP}$ in CTR rats, and causing the appearance of $K_{i\ ATP}$ in HL rats. However, the response of HL animals concerning V_{max} and $K_{m\ ATP}$ was lower than that of CTR animals. (Figure 10**B**, **C**, **D**).

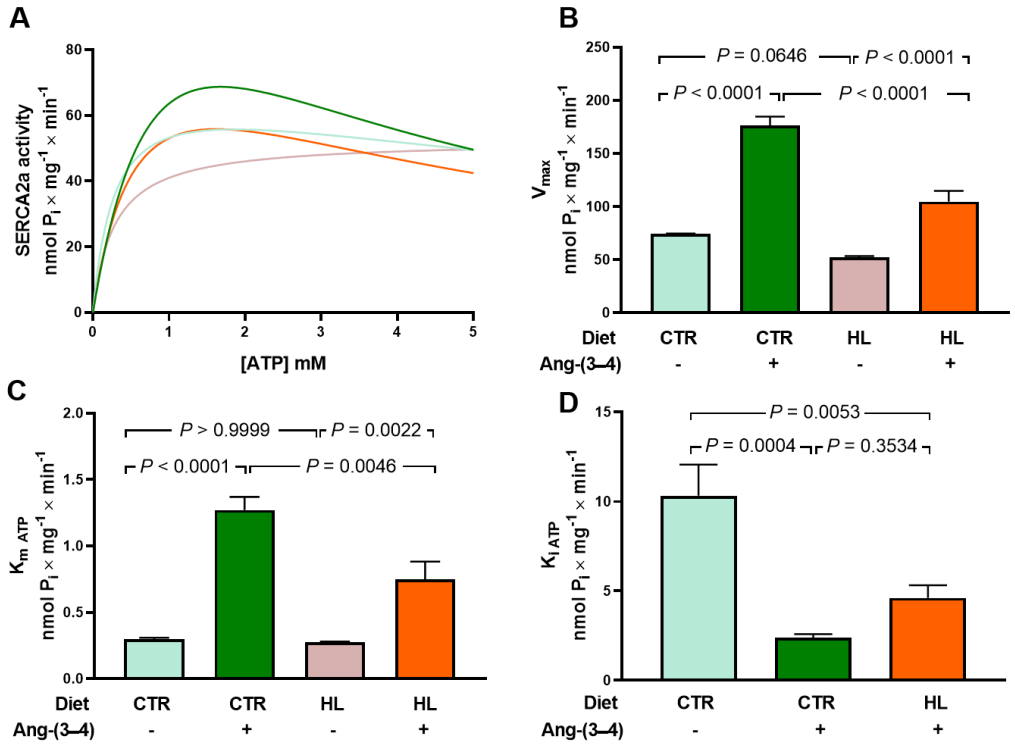

Figure 10. Abnormal kinetics of sarco-endoplasmic reticulum Ca^{2+}-ATPase (SERCA2a) in microsomes of left ventricle cardiomyocytes from overweight rats: partial recovery of the control ATP concentration dependence in Ang-(3–4)-treated overweight animals. (**A**) Simulations of ATP concentration dependence of SERCA2a between 0.1 and 5 mM using experimental mean values of enzyme velocity (n = 5 different microsome preparations). The curves were generated using equations 1 or 2 (see text). Blue, CTR; pink, HL; green, CTR + Ang-(3–4); orange, HL + (Ang-(3–4). (**B**) V_{max} values (nmol $P_i \times mg^{-1} \times min^{-1}$). (**C**) $K_{m\ ATP}$ (mM). (**D**) $K_{i\ ATP}$ (mM). In **B**, **C**, and **D**, bars show mean ± SEM (n = 4–5). Combinations of diets and treatment or not with Ang-(3–4) are indicated on the abscissae. Differences were assessed using two-way ANOVA followed by Bonferroni's test (**B**, **C**) and one-way ANOVA followed Bonferroni's test for selected pairs (**D**); p values are indicated within the panels.

2.6. There Is no Structural Remodeling in Overweight Rats at Juvenile Age

Figure 11 presents the results of echocardiographic studies designed to investigate whether there are indicators of structural remodeling of the left ventricle in moderately overweight and hypertensive rats. Measurements of the internal diameters of the left ventricle at the end of diastole and systole, as well as of the left ventricular end-diastolic and end-systolic volumes, were recorded at the level of the region where the papillary muscles are located (red lines and circles). These measurements (representative recordings in panels **A**, **B**, **C**, and **D**, respectively) demonstrate that HL rats do not present changes in the fractional shortening (Figure 11**D**) or the ejection fraction (Figure 11**E**) and that there were no effects of Ang-(3–4).

 doi:10.20944/preprints202407.1120.v1

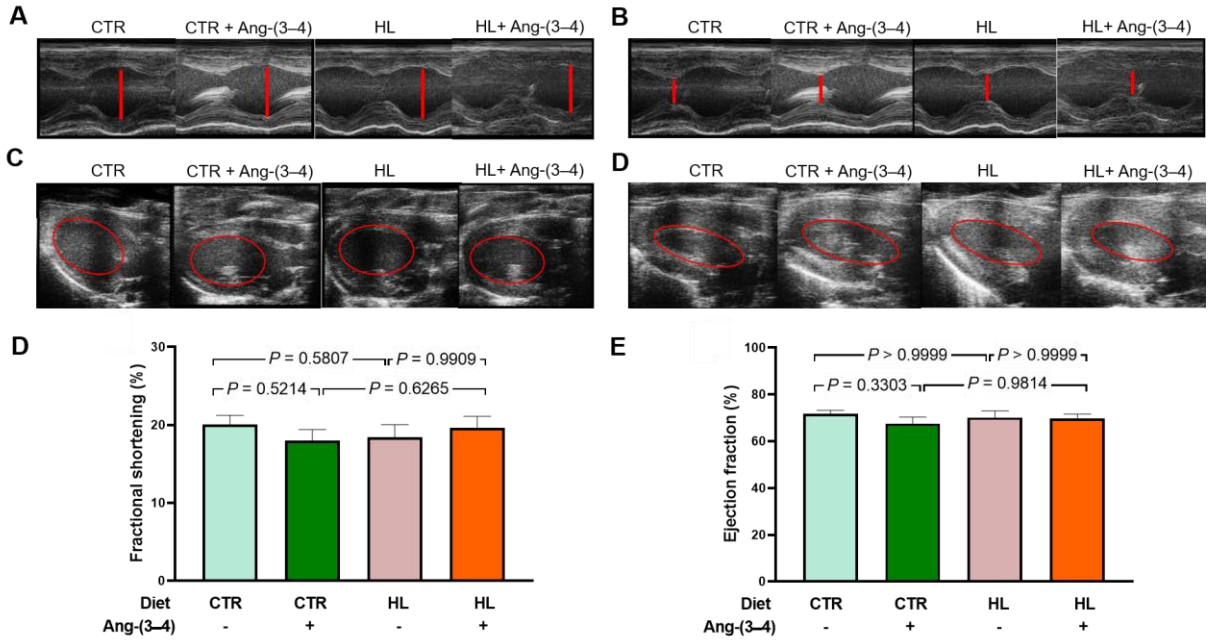

Figure 11. Echocardiography at day 106 reveals still unchanged structural and functional parameters of the left ventricle behind the metabolic, cellular and molecular changes found in overweight rats. Measurements of the left ventricular internal diameter at the end of the diastole (LVIDd) and the end of the systole (LVIDs) allowed calculation of the fractional shortening (FS). Measurements of the left ventricular end-diastolic volume (EDV) and end-systolic volume (ESV) allowed calculation of ejection fraction (EF). Representative echographic recordings of LVIDd (**A**) and LVIDs (**B**). Representative echographic recordings of EDV (**C**) and ESV (**D**). (**E**) Fractional shortening calculated as FS (%) = [(LVIDd - LVDIs)/LVIDd] × 100. (**F**) Ejection fraction calculated as EF (%) = [(EDV - ESV)/EDV] × 100. Bars represent mean ± SEM, which were compared using two-way ANOVA followed by Bonferroni's test (n = 12–17 rats); *p* values are shown within the panels. Combinations of diets and treatment or not with Ang-(3–4) are indicated above the images and on the abscissae of the graphic representations.

3. Discussion

The main findings of the present work are that moderate overweight (Figure 1) in young rats [13] chronically fed a high-fat and high-caloric diet [14] (HL) present – in addition to the gradually installed arterial hypertension – changes in central areas that regulate thirst [32] since liquid intake is markedly lower and, consequently, urinary excretion (Figure 3). A marked and puzzling decrease in plasma triglyceride levels appears to be associated with the non-alcoholic steatosis these rats present [27]. Evidence of the role of upregulation of the RAAS axis coupled to Ang II type 1 receptors (AT_1R) in the left ventricle arises from the observation that increased levels of the pro-inflammatory cytokines IL-6 and TNF-α return to normal values by administering Ang-(3–4) to upregulate signaling coupled to type 2 Ang II receptors (AT_2R). The participation of RAAS also emerges from the observation that, in the myocardium of HL rats, the decrease in $(Na^+ + K^+)$ATPase and the increase in the ouabain-resistant Na^+-ATPase are also normalized by Ang-(3–4), as well as the dependence on ATP concentration characterized by inhibition by excess substrate of the sarco-endoplasmic reticulum Ca^{2+}-ATPase, which was lost in HL rats. However, the important metabolic alterations and notable changes in ion transport ATPases from overweight rats still coexist with fractional shortening and ejection fraction preservation.

Although moderate, the overweight of HL rats is accompanied by a significant increase in visceral fat around the epididymis and in the perirenal region, an observation accompanied by evidence of hyperactivity of the local RAAS coupled with AT_1R. Supporting this idea is the observation that the acute administration of just 4 doses of Ang-(3-4) in the short space of 48 h to antagonize AT_2R-coupled signaling partially reverses the expansion of these biomarkers of increased

 doi:10.20944/preprints202407.1120.v1

visceral fat in HL rats, without any effect in CTR rats (Figure 4). This selective sensitivity indicates the existence of a pro-hypertensive tissue microenvironment [12,17] with upregulation of the Ang II → AT_1R axis. In light of this set of findings, it could be proposed – in terms of mechanisms – that the abnormal activation of this axis would promote lipogenesis in HL rats [33–35], while the allosteric activation [16] of the antagonist Ang II → AT_2R pathway would restore lipase-mediated catalysis in adipocytes [34–36].

The existence of an intense inflammatory state – stimulated by the Ang II → AT_1R pathway – that reaches the heart is confirmed by observations related to the levels of pro-inflammatory cytokines in the left ventricular tissue (Figure 5), which doubled in HL rats, being normalized by Ang-(3–4). We chose to investigate IL-6 due to its known effect on establishing insulin resistance associated with obesity [24] and because it is considered a predictor of mortality in cardiorenal syndromes [37]. The upregulation of TNF-α levels in the left ventricle, in turn, reveals the existence of a link between a process of local inflammation caused by Ang II and subsequent fibrosis due to the differentiation of monocytes into fibroblasts [38], in route to organ remodeling with congestive heart failure [39]. In this context, the significant increase in IL-6 in CTR rats caused by Ang-(3–4) deserves special discussion in the context of the dual effects of this cytokine [40,41]. In normonourished animals Ang-(3–4) would increase the release of the cytokine to exert anti-inflammatory effects, promoting the alternative activation of macrophages to the M2 phenotype [42]. This activation would occur in tissue conditions where intracellular mediators favor IL-6 *trans*-signaling [41,43], e.g. a physiological status of the local RAAS [44].

A metabolic syndrome associated with moderate overweight in HL rats is evidenced by the lipidogram and blood glucose profiles indicating insulin resistance (Figures 6 and 7). The biochemical remodeling of plasma lipoproteins with a decrease in HDL and an increase in LDL is classically described for the dyslipidemias of metabolic syndrome, representing a global metabolic effect of insulin resistance [45,46], which correlates with the increase in visceral fat described above and with the changes in fatty acid fluxes and lipid deposits in the liver found in the hepatocardiorenal syndrome of HL rats [27]. The maintenance of total cholesterol in the HL group at CTR levels would probably results, in turn, from the combination of changes in lipid metabolism in different tissues that compensate for each other and reverberate in the plasma [47]. The marked and atypical decrease in plasma triglycerides could also be linked to the pronounced hepatic steatosis that ultrasound reveals in HL rats [27].

The components of metabolic syndrome with insulin resistance in HL rats, which has the augmented production of cytokines by the visceral fat as a central physiopathogenic factor [48,49], are completed with fasting hyperglycemia and glucose intolerance, completing a network of processes and mechanisms that associate visceral adiposity, insulin resistance, hypertension, changes in body Na^+, and cardiovascular risk [12,50]. Although fasting hyperglycemia and insulin resistance are mild in the HL group, it should be noted that these are young rats. Juvenile obesity, in addition to leading to a progressive worsening of insulin resistance over time, significantly increases cardiovascular risk in adulthood, as demonstrated by the evaluation and comparison of different circulatory parameters in humans [51].

The inflammatory state of the myocardial tissue that the cytokines revealed and the incipient fibrosis process [27] indicate RAAS hyperactivity. This hyperactivity would result from the selective increase/decrease of targets in steps after the binding of Ang II to AT_1R (and a decrease in signaling coupled to AT_2R), because the abundance of both receptors in the left ventricle microsomal fraction remained similar in the 4 groups as shown in Figure 8. Well-known targets downstream of Ang II binding to AT_1R are MAP kinases (ERK1/2, JNK, p38, MAPK), NADPH oxidase (which would lead to increased production of reactive O_2 species) [52,53], PKC (upregulated) and PKA (downregulated) [54,55]. This ensemble, associated with various processes, can be expanded by considering protein kinases involved in cardiac inflammation and remodeling. These altered Ang II → AT_1R and/or Ang II → AT_2R signaling could likely be present in HL rats.

The impact of overweight on Na^+-transporting ATPases (Figure 9) and SERCA2a (Figure 10) also constitutes a central element in the pathophysiology of cardiac structural and functional changes that

 doi:10.20944/preprints202407.1120.v1

can occur in HL rats. Na^+-transporting ATPases because they participate in events related to electrical activity and are involved in dysfunctions described in cardiometabolic diseases [56]. Downregulation of (Na^++K^+)ATPase potentiates apoptosis in cardiomyocytes [57] and oxidative damage [58], which would be especially critical when ROS production is increased by activation of the Ang II → AT_1R axis [59]. Regarding the ouabain-resistant Na^+-ATPase, its functioning in normonourished rats contributes to normal electrical activity [54]. The upregulation of this Na^+ pump due to RAAS hyperactivity in overweight rats could lead to changes in the regulation of cardiomyocyte volume [60] and, therefore, in the function of these cells as a whole [61].

The relevance of potential changes in SERCA2a in HL rats emerges from the fact that its changes impact the contractile process in heart failure [62]. As seen in Figure 10, there are no differences in SERCA2a activity at 5 mM ATP, a concentration close to that encountered in cardiomyocytes in both contraction and relaxation [31]. Mitochondria replenish cytosolic ATP at a rate appropriate to its consumption during contraction [63,64]. The fact that there is a difference in low concentrations of ATP makes it evident that if myocardial inflammatory damage [65] in overweight is accentuated to the point of compromising mitochondrial function [66], the activity of SERCA2a will also be affected. A SERCA2a dysfunction that leads to decreased activity would accelerate the progression to heart failure [67,68] in HL rats. Concerning the stimulation by Ang-(3–4), the fact that the response in HL rats was smaller than in CTR rats suggests that chronic administration of the high-fat diet affected the ability of the Ang II → AT_2R axis to counter-regulate the Ang II → AT_1R axis and therefore some of the changes resulting from the activation of the latter. At this point, it is important to discuss the recovery of the kinetics of SERCA2a inhibition by excess substrate, one of the finest mechanisms of key enzyme activity [69,70]. Inhibition of SERCA2a activity by high ATP makes it sensitive to energy demand during systolic sarcomere contraction during [71]. Thus, its loss in HL rats, recovered by the administration of Ang-(3–4), again indicates a pathological effect at the molecular level resulting from the upregulation of the Ang II → AT_1R axis of the RAAS, which is counterbalanced by the activation of the Ang II → AT_2R axis. In terms of injury mechanisms, it could be that high tissue levels of ROS found in overweight/obesity [8] would be responsible for structural and functional changes in SERCA2a due to the oxidation of cysteines and the nitration of tyrosines [72], which are key amino acids in the enzyme catalysis domains [73].

Although the relationship between obesity and heart failure has been the subject of an increasing number of studies in recent years (for an illustrative review, see [74]), two questions have not yet been answered. They are: (1) Can moderate overweight be associated with or precede early heart failure? (2) What are the effects of inflammation and changes in ion transport in myocardial tissue associated with overweight/obesity? Cardiometabolic diseases in obesity, in which there is an important component of generalized inflammation, evolve and worsen when there is hypertension [75,76]. HL rats became progressively hypertensive throughout the exclusive administration of the high-fat diet [12] and presented myocardial fibrosis [27] despite being moderately overweight. This ensemble of observations adds to the changes in renal Ang II receptors already described [12]. They allow us to propose that the triad known as cardiovascular-kidney-metabolic syndrome [77] should even include moderate weight gains, which, as in the case of HL rats, already have a significant expansion of visceral adiposity. In this initial stage of the evolution of fat mass and cellular and molecular changes in the myocardium, including marked inflammation and important changes in ionic transporters involved in excitation/contraction coupling, there is still no evidence of systolic dysfunction. As shown in Figure 11, both shortening fraction and ejection fraction, which are central measures of left ventricular systolic function [78–80], are preserved. Ang-(3–4) was also without effect, probably because the downstream upregulation of the Ang II → AT_1R axis, discussed above, has not yet reached the macroscopic structural remodeling that echocardiography can reveal.

 doi:10.20944/preprints202407.1120.v1

4. Materials and Methods

4.1. Ethical Considerations

All experimental procedures were approved by the Ethics Committee for Using Animals in Research at the Federal University of Rio de Janeiro under protocol number 075.19. The execution of these procedures adhered to the Committee's Guidelines, which follow the Uniform Requirements for Manuscripts Submitted to Biomedical Journals established by the International Committee of Medical Journal Editors and the ARRIVE guidelines [81].

4.2. Experimental Groups and Diets

At birth, the rats were distributed so that each mother remained with 8 animals, ensuring that all had equal nutritional access [82]. All male animals were preserved, and, if necessary, the maximum number of offspring per mother was supplemented with females. The animals were weaned on day 21 of life, started to receive a commercial diet for rodents (Neovia Animal Nutrition, Contagem, Brazil), and were regrouped to avoid the litter effect [83] in cages containing 5 animals until the 57 days of life in a controlled environment at 23 ± 2 °C with a 12 h/12 h light and dark cycle.

Upon reaching 58 days of life, the animals were randomly separated into 2 groups. The control (CTR), with free access to a diet containing 36, 292, and 57 kcal/100 g dry weight chow from lipids, carbohydrates, and proteins, respectively, totaling 385 kcal/100 g. The high lipid (HL) group received 402, 103, and 69 kcal/100 g from lipids, carbohydrates, and proteins, respectively [14]. The Na^+ content, measured by flame photometry, varied between 5.1–5.8 and 7.7–8.0 mequiv/100 g dry chow (CTR and HL, respectively) [12]. For greater detail on the diets, see Supplement Table S1 in [12]. Both groups had free access to filtered water. Both CTR and chow HL food were purchased from PragSoluções (Jaú, Brazil). Upon reaching 104 days of diet (162 days of age), the rats were separated into 2 more groups – also randomly – and housed individually in metabolic cages so that half received by gavage 4 doses (80 mg/kg body mass diluted in water) of Ang-(3–4) (AminoTech, Sorocaba, Brazil). Untreated rats received only the vehicle.

After 48 days of treatment, the rats were sacrificed by decapitation. Each animal's heart, perirenal, and epididymal fat were immediately collected using surgical scissors. The organs were dried with filter paper to remove excess blood and weighed. Perirenal and epididymal fat masses were considered markers of visceral fat [22], as described above.

4.3. Lipidogram

After 70 days of consumption of the CTR or HL diets (128 days of life), the rats were fasted for 10 h (water *ad libitum*) and anesthetized after this period with ethyl ether. Blood was collected by caudal puncture, centrifuged at 13,000× g for 5 min, and plasma was collected to measure total cholesterol/TC, HDL cholesterol, and triglycerides/TG. Commercial kits (Bioclin, Belo Horizonte, Brazil) were used: Bioclin K083 mono reagent total cholesterol, Bioclin enzymatic HDL cholesterol, and Bioclin K117 mono reagent triglycerides.

4.4. Glycemia Determination and Oral Glucose Tolerance Curve

After 95 days of diet (153 days of age), some of the animals that received the CTR or HL diets were fasted for 10 h (water *ad libitum*) to measure blood glucose. Immediately afterward, they received 2 g of glucose/kg body mass by gavage. The blood glucose measurement was done using the touch-ultra mini glucometer (OneTouch®-LifeScan, Milpitas, CA, USA), taking the fasting blood glucose value to construct the curve (time zero). The measurements were taken 15, 30, 50, 60, and 120 min apart.

4.5. Preparation of Left Ventricle Microsomes

After sacrifice (at 106 days of exposure to CTR or HL diets, 164 days of life), the heart of each animal was immersed in a solution containing 250 mM sucrose, 1 mM imidazole, 1 mM EDTA, and

 doi:10.20944/preprints202407.1120.v1

0.15 mg/mL of trypsin inhibitor (pH adjusted to 7.6 with TRIS) [84]. Each heart was carefully dissected to obtain the left ventricle, weighed, and cut into smaller fragments with the aid of surgical scissors. A pool of 2–3 ventricles was suspended in the same solution (1 g of tissue in 4 mL).

The suspension was mechanically homogenized at 4 °C using a Potter Elvejhem homogenizer with a Teflon pestle (5 cycles of 1 min at 1,700 rpm with 10 s pauses). Homogenates were sequentially centrifuged twice (1,650× *g* for 15 min at 4 °C, 70 Ti Beckman rotor) to remove debris and nuclei and then the supernatant was centrifuged at 115,000× *g* for 60 min. The resulting precipitate was recovered and suspended in 250 mM sucrose solution and stored in liquid N_2. Protein concentration was determined by the Lowry method [85]. This microsomal fraction has a sarco-endoplasmic reticulum content of 8–10%, which allows simultaneous assessment of (Na^++K^+)ATPase, ouabain-resistant Na^+-ATPase, and sarco-endoplasmic reticulum Ca^{2+}-ATPase 2a (SERCA2a) activities.

4.6. SDS PAGE and Western Blotting

Western blotting evaluated the abundance of (Na^++K^+)ATPase, Ang II receptors, IL-6, and TNFα. Microsome samples (80 µg of protein) were loaded onto a gel containing 10% polyacrylamide and SDS [86]. After the separation and transfer to nitrocellulose membranes (GE Healthcare, Chicago, IL, USA), the membranes were incubated for 1 h in a solution containing 5% skimmed milk powder diluted in Tris-buffered saline (pH 7.6). The membranes were incubated overnight with the corresponding primary antibody, remaining exposed after 1 h, and incubated with the secondary antibody for subsequent development.

The primary antibodies were as follows. Against the α-catalytic subunit of (Na^++K^+)ATPase, the catalog antibody A276 (Sigma-Aldrich, Saint Louis, MO, USA) was used at a dilution of 1:1,000. For the cytokines IL-6 and TNFα, antibodies from Imuny Biotechnology (Campinas, Brazil; catalog IM-0407) at a dilution of 1:1,000 and from Immuny Biotechnology (catalog IM-406) at a dilution of 1:1,000 were used, respectively. For AT_1R, the anti-rabbit polyclonal antibody was used (Alomone Labs, Jerusalem, Israel; catalog AAR-011, at a dilution of 1:500). For AT_2R, the anti-rabbit polyclonal antibody (Santa Cruz Biotechnology, Dallas, TX, USA; catalog SC-9040, dilution 1:250). The secondary antibodies were anti-mouse and anti-rabbit from GE Healthcare (NA934 and NA931, respectively), both at 1:5,000 dilution. The loading control was performed through immunodetection of GAPDH (monoclonal antibody SC-32233, Santa Cruz Biotechnology). The LAS 4000 system equipment (GE Healthcare) and the ImageJ software (NIH) were used to detect the immunosignals.

4.7. Measurement of Left Ventricle Na^+-transporting ATPases Activity

The activity of the two Na^+-transporting ATPases was assessed by measuring the orthophosphate released during ATP hydrolysis [87]. For the (Na^++K^+)ATPase experiments, microsome samples (0.05 mg/mL) were preincubated at 37 °C for 10 min in a solution containing 50 mM Bis-TRIS propane (pH 7.4), 0.2 mM EDTA, 120 mM NaCl, and 5 mM $MgCl_2$, in the absence or presence of 5 mM ouabain. The reaction was started by adding a solution containing 5 mM ATP and 24 mM KCl (final concentrations) and terminated 10 min later by adding a suspension of activated charcoal in 1 N HCl (1 vol:1 vol). For the subsequent colorimetric reaction, the reaction tubes were centrifuged at 13,000x g for 15 min to remove charcoal. Next, the supernatant was removed and mixed with ferrous sulfate-molybdate solution (1 vol:1 vol). (Na^++K^+)ATPase activity was calculated by subtracting the activity obtained in the presence of ouabain from the total activity.

The ouabain-resistant and furosemide-sensitive Na^+-ATPase activity was assessed by first preincubating microsome samples (0.2 mg/mL) in a solution containing 20 mM Hepes-TRIS (pH 7.0), 10 mM $MgCl_2$, 120 mM NaCl, and 2 mM ouabain, in the presence or absence of 2 mM furosemide. The reaction (at 37 °C) was started by adding 5 mM ATP and finished 10 min later, following the process described for the (Na^++K^+)ATPase. The activity of the ouabain-resistant and furosemide-sensitive Na^+-ATPase was determined by the difference between the activities measured in the absence and presence of furosemide.

 doi:10.20944/preprints202407.1120.v1

4.8. Measurement of Left Ventricle Sarco-Endoplasmic Reticulum Ca^{2+}-ATPase/SERCA2a Activity

SERCA2a activity was assayed at increasing ATP concentrations (0.1, 0.2, 0.5, 1, 3 and 5 mM). Microsomes (0.05 mg/mL) were initially preincubated at room temperature for 20 min in the absence or presence of 4.6 μM thapsigargin, in a solution containing 50 mM TRIS-HCl (pH 7.0), 160 mM sucrose, 10 mM NaN_3, 0.2 mM ouabain, 1.0 mM EGTA and sufficient $MgCl_2$ and $CaCl_2$ concentrations [88] to obtain free Mg^{2+} and Ca^{2+} concentrations of 0.5 mM and 20 μM, respectively, for each ATP concentration. After preincubation, ATP was added to obtain the final concentrations mentioned above. After incubation for 15 min at 37 °C, the reaction was stopped by adding the charcoal suspension in acid and the samples processed as in the case of Na^+-transporting ATPases. SERCA2a activity was calculated as the difference between total activity and that obtained in the presence of thapsigargin.

4.9. Echocardiographic Images

Echocardiography studies were performed to evaluate cardiac structure/function in vivo. The studies were conducted using a Vevo 2100 High-Resolution Imaging System (VisualSonics, Toronto, Canada) coupled to a 21 MHz transductor. Rats (aged 164 days; 106 days of exposure to the different diets, including the two days under Ang-(3–4 treatment) were maintained under isoflurane anesthesia during the study. Images were acquired in bidimensional and M mode [89] and then analyzed by a blinded specialist using the VevoLab software.

4.10. Statistical Analysis

Results, which were analyzed using GraphPad Prism 8.0.2, are presented as mean ± SEM. Two means were compared using the paired or unpaired Student's t-test, as described in the captions of each figure. For comparisons between more than two means, 2-way ANOVA was used. Differences were considered significant at $p < 0.05$.

5. Conclusions

In conclusion, our research demonstrates that being very moderately overweight already leads to critical processes of molecular damage in myocardial tissue, which are revealed by inflammatory biomarkers. These accentuated molecular lesions can alter the left ventricle's hemodynamic function, which is still preserved. Future directions of the study point to the challenge of characterizing altered components of signaling pathways downstream of the cardiac Ang II receptors, whose abundance remains unmodified in moderate overweight. At this initial pathological stage, it will be central to detect intervention targets to prevent progression to systolic dysfunction and cardiac remodeling.

Author Contributions: For research articles with several authors, a short paragraph specifying their individual contributions must be provided. The following statements should be used Conceptualization, T.C., R.L., H.M-F., D.B.M. and A.V.; Methodology, T.C., R.L., M.L.L.G., M.A.E.P., G.C-S., D.B.M.; Validation, T.C., R.L. and A.V.; Formal Analysis, T.C., R.L., M.L.L.G., M.A.E.P., D.B.M. and A.V.; Investigation, T.C., R.L., M.L.L.G., M.A.E.P., G.C-S., D.B.M. and A.V.; Resources, T.C., R.L., M.L.L.G., M.A.E.P., H.M-F., G.C-S., D.B.M. and A.V.; Data curation, T.C., R.L., H.M-F., G.C-S., D.B.M. and A.V.; Writing—Original draft, T.C., R.L., H.M-F, D.B.M. and A.V.; Writing—Review and editing, T.C., R.L., H.M-F, D.B.M. and A.V.; Visualization, T.C., R.L., H.M-F, D.B.M. and A.V.; Supervision, T.C. and A.V.; Project Administration, T.C., R.L., G.C-S. and A.V.; Funding Acquisition, A.V. All authors have read and agreed to the published version of the manuscript.

Funding: This research was funded by the Carlos Chagas Filho Rio de Janeiro State Foundation/FAPERJ (grant numbers: E-26/201.909/2020 and E-26/200.866/2021), the National Council for Scientific and Technological Development/CNPq (grant number: 311578/2019-5), and the Coordination for the Improvement of Higher Education Personnel/CAPES (grant numbers: 88887.320213/2019-00 and 88887.623346/2021-00). The APC was funded by the National Council for Scientific and Technological Development/CNPq (grant number 465656/2014-5).

Institutional Review Board Statement: All experimental procedures were approved by the Ethics Committee for Using Animals in Research at the Federal University of Rio de Janeiro under protocol number 075.19. The execution of these procedures adhered to the Committee's Guidelines, which follow the Uniform Requirements

 doi:10.20944/preprints202407.1120.v1

for Manuscripts Submitted to Biomedical Journals established by the International Committee of Medical Journal Editors and the ARRIVE guidelines [81].

Informed Consent Statement: Not applicable.

Data Availability Statement: The data presented in this study are available on request from the corresponding author.

Conflicts of Interest: The authors declare no conflicts of interest. The funders had no role in the design of the study; in the collection, analyses, or interpretation of data; in the writing of the manuscript; or in the decision to publish the results.

References

1. Swinburn, B.A.; Kraak, V.I.; Allender, S.; Atkins, V.J.; Baker, P.I.; Bogard, J.R.; Brinsden, H.; Calvillo, A.; De Schutter, O.; Devarajan, R.; Ezzati, M.; Friel, S.; Goenka, S.; Hammond, R.A.; Hastings, G.; Hawkes, C.; Herrero, M.; Hovmand, P.S.; Howden, M.; Jaacks, L.M.; Kapetanaki, A.B.; Kasman, M.; Kuhnlein, H.V.; Kumanyika, S.K.; Larijani, B.; Lobstein, T.; Long, M.W.; Matsudo, V.K.R.; Mills, S.D.H.; Morgan, G.; Morshed, A.; Nece, P.M.; Pan, A.; Patterson, D.W.; Sacks, G.; Shekar, M.; Simmons, G.L.; Smit, W.; Tootee, A.; Vandevijvere, S.; Waterlander, W.E.; Wolfenden, L.; Dietz, W.H. The global syndemic of obesity, undernutrition, and climate change: the lancet commission report. *Lancet*. **2019**, *393*, 791–846. https://doi.org/10.1016/S0140-6736(18)32822-8
2. World Health Organization (WHO). Obesity and overweight. Available online: https://www.who.int/news-room/fact-sheets/detail/obesity-and-overweight (acessed on june 26, 2024).
3. United Nations (UN). World population to reach 8 billion on 15 November 2022. Available online: https://www.un.org/en/desa/world-population-reach-8-billion-15-november-2022 (acessed on June 26, 2024).
4. Xu, H.; Cupples, L.A.; Stokes, A.; Liu, C.T. Association of obesity with mortality over 24 years of weight history: findings from the framingham heart study. *JAMA Netw. Open*. **2018**, *1*, e184587. https://doi.org/10.1001/jamanetworkopen.2018.4587
5. Singh, A.S.; Mulder, C.; Twisk, J.W.; van Mechelen, W.; Chinapaw, M.J. Tracking of childhood overweight into adulthood: a systematic review of the literature. *Obes. Rev*. **2008**, *9*, 474–488. https://doi.org/10.1111/j.1467-789X.2008.00475.x
6. LeBlanc, A.G.; Katzmarzyk, P.T.; Barreira, T.V.; Broyles, S.T.; Chaput, J.P.; Church, T.S.; Fogelholm, M.; Harrington, D.M.; Hu, G.; Kuriyan, R.; Kurpad, A.; Lambert, E.V.; Maher, C.; Maia, J.; Matsudo, V.; Olds, T.; Onywera, V.; Sarmiento, O.L.; Standage, M.; Tudor-Locke, C.; Zhao, P.; Tremblay, M.S. and ISCOLE Research Group. Correlates of total sedentary time and screen time in 9–11 year-old children around the world: the international study of childhood obesity, lifestyle and the environment. *PLoS One*. **2015**, *10*, e0129622. https://doi.org/10.1371/journal.pone.0129622
7. Goran, M.I. Energy metabolism and obesity. *Med. Clin. N. Am*. **2000**, *84*, 347–362. https://doi.org/10.1016/s0025-7125(05)70225-x
8. Kopp, W. How Western diet and lifestyle drive the pandemic of obesity and civilization diseases. *Diabetes Metab. Syndr. Obes*. **2019**, *12*, 2221–2236. https://doi.org/10.2147/DMSO.S216791
9. Popkin, B.M.; Richards, M.K.; Montiero, C.A. Stunting is associated with overweight in children of four nations that are undergoing the nutrition transition. *J. Nutr*. **1996**, *126*, 3009–3016. https://doi.org/10.1093/jn/126.12.3009
10. Caballero, B.; Rubinstein, S. Environmental factors affecting nutritional status in urban areas of developing countries. *Arch. Latinoam. Nutr*. **1997**, **47**, 3–8.
11. Mill, J.G.; Malta, D.C.; Machado, I.E.; PateI, A.; Pereira, C.A.; Jaime, P.C.; Szwarcwald, C.L.; Rosenfeld, L.G. Estimation of salt intake in the Brazilian population: results from the 2013 National Health Survey. *Rev. Bras. Epidemiol*. **2019**, *22*, e190009. https://doi.org/10.1590/1980-549720190009.supl.2
12. Luzes, R.; Crisóstomo, T.; Silva, P.A.; Iack, R.; de Abreu V.G.; Francischetti E.A.; Vieyra, A. Angiotensin-(3–4) normalizes blood pressure, decreases Na^+ and energy intake, but preserves urinary Na^+ excretion in overweight hypertensive rats. Biochim. Biophys. *Acta Mol. Basis Dis*. **2021**, *1867*, 166012. https://doi.org/10.1016/j.bbadis.2020.166012
13. Quinn R. Comparing rat's to human's age: how old is my rat in people years? *Nutrition*. **2005**, *21*, 775–777. https://doi.org/10.1016/j.nut.2005.04.002
14. Touati, S.; Meziri, F.; Devaux, S.; Berthelot, A.; Touyz, R.M.; Laurant, P. Exercise reverses metabolic syndrome in high-fat diet-induced obese rats. *Med. Sci. Sports Exerc*. **2011**, *43*, 398–407. https://doi.org/10.1249/MSS.0b013e3181eeb12d
15. Paul, M., Mehr. A.P., Kreutz R. Physiology of local renin-angiotensin systems. *Physiol. Rev*. **2006**, *86*, 747–803. https://doi.org/10.1152/physrev.00036.2005

16. Axelband, F.; Dias, J.; Miranda, F.; Ferrão, F.M.; Reis, R.I.; Costa-Neto, C.M.; Lara, L.S.; Vieyra, A. Angiotensin-(3–4) counteracts the Angiotensin II inhibitory action on renal Ca^{2+}-ATPase through a cAMP/PKA pathway. *Regul. Pept*. **2012**, *177*, 27–34. https://doi.org/10.1016/j.regpep.2012.04.004
17. Dias, J.; Ferrão, F.M.; Axelband, F.; Carmona, A.K.; Lara, L.S.; Vieyra, A. ANG-(3–4) inhibits renal Na^{+}-ATPase in hypertensive rats through a mechanism that involves dissociation of ANG II receptors, heterodimers, and PKA. *Am. J. Physiol. Renal Physiol*. **2014**, *306*, F855–F863. https://doi.org/10.1152/ajprenal.00488.2013
18. Dias, J.; Axelband, F.; Lara, L.S.; Muzi-Filho, H.; Vieyra, A. Is angiotensin-(3–4) (Val-Tyr). the shortest angiotensin II-derived peptide. opening new vistas on the renin-angiotensin system? *J. Renin. Angiotensin. Aldosterone Syst*. **2017**, *18*, 1470320316689338. https://doi.org/10.1177/1470320316689338
19. Reeves, P.G. Components of the AIN-93 diets as improvements in the AIN-76A diet. *J. Nutr*. **1997**, *127*, 838S–841S. https://doi.org/10.1093/jn/127.5.838S
20. Ziegler, A.A.; Grobe, C.C.; Reho, J.J.; Jensen, E.S.; Thulin, J.D.; Segar, J.L.; Grobe, J.L. Short-term housing in metabolic caging on measures of energy and fluid balance in male C57BL/6J mice (*Mus musculus*). *J. Am. Assoc. Lab. Anim. Sci*. **2022**, *61*, 132–139. https://doi.org/10.30802/AALAS-JAALAS-21-000087
21. Chughtai, H.L.; Morgan, T.M.; Rocco, M.; Stacey, B.; Brinkley, T.E.; Ding, J.; Nicklas, B.; Hamilton, C.; Hundley, W.G. Renal sinus fat and poor blood pressure control in middle-aged and elderly individuals at risk for cardiovascular events. *Hypertension*. **2010**, *56*, 901–906. https://doi.org/10.1161/HYPERTENSIONAHA.110.157370
22. Chusyd, D.E.; Wang, D.; Huffman, D.M.; Nagy, T.R. Relationships between rodent white adipose fat pads and human white adipose fat depots. *Front. Nutr*. **2016**, *3*, 10–22. https://doi.org/10.3389/fnut.2016.00010
23. Kim, Y.J.; Park, T. Genes are differentially expressed in the epididymal fat of rats rendered obese by a high-fat diet. *Nutr. Res*. **2008**, *28*, 414–422. https://doi.org/10.1016/j.nutres.2008.03.015
24. Kern, P.A.; Ranganathan, S.; Li, C.; Wood, L.; Ranganathan, G. Adipose tissue tumor necrosis factor and interleukin-6 expression in human obesity and insulin resistance. *Am. J. Physiol. Endocrinol. Metab*. **2001**, *280*, E745–E751. https://doi.org/10.1152/ajpendo.2001.280.5.E745
25. Yu, J.Y.; Choi, W.J.; Lee, H.S.; Lee, J.W. Relationship between inflammatory markers and visceral obesity in obese and overweight Korean adults: An observational study. *Medicine*. **2019**, *98*, e14740. https://doi.org/10.1097/MD.0000000000014740
26. Kolb H. Obese visceral fat tissue inflammation: from protective to detrimental? *BMC Med*. **2022**, *20*, 494. https://doi.org/10.1186/s12916-022-02672-y
27. Crisóstomo, T.; Pardal, M.A.E.; Herdy, S.A.; Muzi-Filho, H.; Mello, D.B.; Takiya, C.M.; Luzes, R.; Vieyra, A. Liver steatosis, cardiac and renal fibrosis, and hypertension in overweight rats: Angiotensin-(3–4)-sensitive hepatocardiorenal syndrome. *Metabol. Open*. **2022**, *14*, 100176. https://doi.org/10.1016/j.metop.2022.100176
28. Friedewald, W.T.; Levy, R.I.; Fredrickson, D.S. Estimation of the concentration of low-density lipoprotein cholesterol in plasma, without use of the preparative ultracentrifuge. *Clin. Chem*. **1972**, *18*, 499−502.
29. Pinz, I.; Tian, R.; Belke, D.; Swanson, E.; Dillmann, W.; Ingwall, J.S. Compromised myocardial energetics in hypertrophied mouse hearts diminish the beneficial effect of overexpressing SERCA2a. *J. Biol. Chem*. **2011**, *286*, 10163–10168. https://doi.org/10.1074/jbc.M110.210757
30. Yoshino, M.; Murakami, K. Analysis of the substrate inhibition of complete and partial types. *SpringerPlus*. **2015**, *4*, 292. https://doi.org/10.1186/s40064-015-1082-8
31. Michailova, A.; McCulloch, A. Model study of ATP and ADP buffering, transport of Ca^{2+} and Mg^{2+}, and regulation of ion pumps in ventricular myocyte. *Biophys. J*. **2001**, *81*, 614–629. https://doi.org/10.1016/S0006-3495(01)75727-X
32. Li, Z.; Iwai, M.; Wu, L.; Shiuchi, T.; Jinno, T.; Cui, T.X.; Horiuchi, M. Role of AT2 receptor in the brain in regulation of blood pressure and water intake. *Am. J. Physiol. Heart Circ. Physiol*. **2003**, *284*, H116–H121. https://doi.org/10.1152/ajpheart.00515.2002
33. Wellen, K.E.; Hotamisligil, G.S. Inflammation, stress, and diabetes. *J. Clin. Invest*. **2005**, *115*, 1111–1119. https://doi.org/10.1172/JCI25102
34. Pérez-Torres, I.; Gutiérrez-Alvarez, Y.; Guarner-Lans, V.; Díaz-Díaz, E.; Manzano Pech, L.; Caballero-Chacón, SDC. Intra-abdominal fat adipocyte hypertrophy through a progressive alteration of lipolysis and lipogenesis in metabolic syndrome rats. *Nutrients*. **2019**, *11*, 1529. https://doi.org/10.3390/nu11071529
35. Yang, Y.; Fu, M.; Li, M.D.; Zhang, K.; Zhang, B.; Wang, S.; Liu, Y.; Ni, W.; Ong, Q.; Mi, J.; Yang, X. O-GlcNAc transferase inhibits visceral fat lipolysis and promotes diet-induced obesity. *Nat. Commun*. **2020**, *11*, 181. https://doi.org/10.1038/s41467-019-13914-8
36. Langin, D.; Dicker, A.; Tavernier, G.; Hoffstedt, J.; Mairal, A.; Rydén, M.; Arner, E.; Sicard, A.; Jenkins, C. M.; Viguerie, N.; van Harmelen, V.; Gross, R.W.; Holm, C.; Arner, P. Adipocyte lipases and defect of lipolysis in human obesity. *Diabetes*. **2005**, *54*, 3190–3197. https://doi.org/10.2337/diabetes.54.11.3190

37. Clementi, A.; Brocca, A.; Virzì, G.M.; de Cal, M.; Giavarina, D.; Carta, M.; Muciño-Bermejo, M.J.; Hinna, D.T.; Salvador, L.; Ronco, C. Procalcitonin and interleukin-6 levels: are they useful biomarkers in cardiac surgery patients? *Blood Purif*. **2017**, *43*, 290–297. https://doi.org/10.1159/000454672
38. Duerrschmid, C.; Crawford, J.R.; Reineke, E.; Taffet, G.E.; Trial, J.; Entman, M.L.; Haudek S.B. TNF receptor 1 signaling is critically involved in mediating angiotensin-II-induced cardiac fibrosis. *J. Mol. Cell. Cardiol*. **2013**, *57*, 59–67. https://doi.org/10.1016/j.yjmcc.2013.01.006
39. Bradham, W.S.; Bozkurt, B.; Gunasinghe, H.; Mann, D.; Spinale, F.G. Tumor necrosis factor-alpha and myocardial remodeling in progression of heart failure: a current perspective. *Cardiovasc. Res*. **2002**, *53*, 822–830. https://doi.org/10.1016/s0008-6363(01)00503-x
40. Fuster, J.J.; Walsh, K. The good, the bad, and the ugly of interleukin-6 signaling. *EMBO J*. **2014**, *33*, 1425–1427. https://doi.org/10.15252/embj.201488856
41. Forcina, L.; Franceschi, C.; Musarò A. The hormetic and hermetic role of IL-6. *Ageing Res. Rev*. **2022**, *80*, 101697. https://doi.org/10.1016/j.arr.2022.101697
42. Mauer, J., Chaurasia, B., Goldau, J., Vogt, M.C., Ruud, J., Nguyen, K.D., Theurich, S., Hausen, A.C., Schmitz, J., Brönneke, H.S., Estevez, E., Allen, T.L., Mesaros, A., Partridge, L., Febbraio, M.A., Chawla, A., Wunderlich, F.T., Brüning, J.C. Signaling by IL-6 promotes alternative activation of macrophages to limit endotoxemia and obesity-associated resistance to insulin. *Nat. Immunol*. **2014**, *15*, 423–430. https://doi.org/10.1038/ni.2865
43. Scheller, J.; Chalaris, A., Schmidt-Arras, D.; Rose-John, S. The pro- and anti-inflammatory properties of the cytokine interleukin-6. *Biochim. Biophys. Acta*. **2011**, *1813*, 878–888. https://doi.org/10.1016/j.bbamcr.2011.01.034
44. De Mello, W.C. Local renin angiotensin aldosterone systems and cardiovascular diseases. *Med. Clin. North Am*. **2017**, *101*, 117–127. https://doi.org/10.1016/j.mcna.2016.08.017
45. Chan, D.C.; Barrett, P.H.; Watts, G.F. Lipoprotein kinetics in the metabolic syndrome: pathophysiological and therapeutic lessons from stable isotope studies. *Clin. Biochem. Rev*. **2004**, *25*, 31–48.
46. Rizzo, M.; Berneis, K. An update on the role of the quality of LDL in cardiovascular risk: the contribution of the universities of Palermo and Zurich. *Recent Pat. Cardiovasc. Drug Discov*. **2007**, *2*, 85–88. https://doi.org/10.2174/157489007780832489
47. Rashid, S.; Genest, J. Effect of obesity on high-density lipoprotein metabolism. *Obesity*. **2007**, *15*, 2875–2888. https://doi.org/10.1038/oby.2007.342
48. Garbarino, J.; Sturley, S.L. Saturated with fat: new perspectives on lipotoxicity. *Curr Opin. Clin. Nutr. Metab. Care*. **2009**, *12*, 110–116. https://doi.org/10.1097/MCO.0b013e32832182ee
49. Caër, C.; Rouault, C.; Le Roy, T.; Poitou, C.; Aron-Wisnewsky, J.; Torcivia, A.; Bichet, J.C.; Clément, K.; Guerre-Millo, M.; André, S. Immune cell-derived cytokines contribute to obesity-related inflammation, fibrogenesis and metabolic deregulation in human adipose tissue. *Sci. Rep*. **2017**, *7*, 3000. https://doi.org/10.1038/s41598-017-02660-w
50. Strazzullo, P.; Barbab, G.; Cappuccioc, F.P.; Sianib, A.; Trevisand, M.; Farinaroe, E.; Paganoa, E.; Barbatoa, A.; Iaconea, R.; Galletti, F. Altered renal sodium handling in men with abdominal adiposity: a link to hypertension. *J. Hypertens*. **2001**, *19*, 2157–2164. https://doi.org/10.1097/00004872-200112000-00007
51. Nadeau, K.J.; Maahs, D.M.; Daniels, S.R.; Eckel, R.H. Childhood obesity and cardiovascular disease: links and prevention strategies. *Nat. Ver. Cardiol*. **2011**, *8*, 513–525. https://doi.org/10.1038/nrcardio.2011.86
52. Mehta, P.K.; Griendling, K.K. Angiotensin II cell signaling: physiological and pathological effects in the cardiovascular system. *Am. J. Physiol. Cell Physiol*. **2007**, *292*, C82–C97. https://doi.org/10.1152/ajpcell.00287.2006
53. Ranjit, A.; Khajehpour, S.; Aghazadeh-Habashi, A. Update on angiotensin II subtype 2 receptor: focus on peptide and nonpeptide agonists. *Mol. Pharmacol*. **2021**, *99*, 469–487. https://doi.org/10.1124/molpharm.121.000236
54. Silva, P. A.; Monnerat-Cahli, G.; Pereira-Acácio, A.; Luzardo, R.; Sampaio, L.S.; Luna-Leite, M.A.; Lara, L.S.; Einicker-Lamas, M.; Panizzutti, R.; Madeira, C.; Vieira-Filho, L.D.; Castro-Chaves, C.; Ribeiro, V.S.; Paixão, A.D.O.; Medei, E.; Vieyra, A. Mechanisms Involving Ang II and MAPK/ERK1/2 signaling pathways underlie cardiac and renal alterations during chronic undernutrition. *PLoS One*. **2014**, *9*, e100410. https://doi.org/10.1371/journal.pone.0100410
55. Silva, P.A.; Muzi-Filho, H.; Pereira-Acácio, A.; Dias, J.; Martins, J.F.; Landim-Vieira, M.; Verdoorn, K.S.; Lara, L.S.; Vieira-Filho, L.D.; Cabral, E.V.; Paixão, A.D.; Vieyra, A. Altered signaling pathways linked to angiotensin II underpin the upregulation of renal Na^+-ATPase in chronically undernourished rats. *Biochim. Biophys. Acta*. **2014**, *1842*, 2357–2366. https://doi.org/10.1016/j.bbadis.2014.09.017
56. Obradovic, M.; Sudar-Milovanovic, E.; Gluvic, Z.; Banjac, K.; Rizzo, M.; Isenovic, E.R. The Na^+/K^+-ATPase: A potential therapeutic target in cardiometabolic diseases. *Front. Endocrinol. (Lausanne)*. **2023**, *14*, 1150171. https://doi.org/10.3389/fendo.2023.1150171
57. Liu, C.; Bai, Y.; Chen, Y.; Wang, Y.; Sottejeau, Y.; Liu, L.; Li, X.; Lingrel, J.B.; Malhotra, D.; Cooper, C.J; Shapiro, J.I.; Xie, Z.J.; Tian, J. Reduction of Na/K-ATPase potentiates marinobufagenin-induced cardiac

dysfunction and myocyte apoptosis. *J. Biol. Chem*. **2012**, *287*, 16390–16398. https://doi.org/10.1074/jbc.M111.304451

58. Hua, F.; Wu, Z.; Yan, X.; Zheng, J.; Sun, H.; Cao, X.; Bian, J.S. DR region of Na^+-K^+-ATPase is a new target to protect heart against oxidative injury. *Sci. Rep*. **2018**, *8*, 13100. https://doi.org/10.1038/s41598-018-31460-z
59. Cat, A.N.D.; Montezano, A.C.; Burger, D.; Touyz, R.M. Angiotensin II, NADPH oxidase, and redox signaling in the vasculature. *Antioxid. Redox Signal*. **2013**, *19*, 1110-1120. https://doi.org/10.1089/ars.2012.4641
60. Camejo, J.L.; Proverbio, T.; Proverbio, F. Ouabain-insensitive, Na^+-stimulated ATPase activity in rabbit cardiac sarcolemma. *Comp. Biochem. Physiol. B Biochem. Mol. Biol*. **1995**, *110*, 345–348. https://doi.org/10.1016/0305-0491(94)00150-s
61. Carlsson, M.; Cain, P.; Holmqvist, C.; Stahlberg, F.; Lundback, S.; Arheden, H. Total heart volume variation throughout the cardiac cycle in humans. *Am. J. Physiol. Heart Circ. Physiol*. **2004**, *287*, H243–H250. https://doi.org/10.1152/ajpheart.01125.2003
62. Park, W.J.; Oh, J.G. SERCA2a: a prime target for modulation of cardiac contractility during heart failure. *BMB Rep*. **2013**, *46*, 237–243. https://doi.org/10.5483/bmbrep.2013.46.5.077
63. Brown, G.C. Control of respiration and ATP synthesis in mammalian mitochondria and cells. *Biochem. J*. **1992**, *284*, 1–13. https://doi.org/10.1042/bj2840001
64. Bell, C.J.; Bright, N.A.; Rutter, G.A.; Griffiths, E.J. ATP regulation in adult rat cardiomyocytes: time-resolved decoding of rapid mitochondrial calcium spiking imaged with targeted photoproteins. *J. Biol. Chem*. **2006**, *281*, 28058–28067. https://doi.org/10.1074/jbc.M604540200
65. Jia, L.; Li, Y.; Xiao, C.; Du, J. Angiotensin II induces inflammation leading to cardiac remodeling. *Front. Biosci*. **2012**, *17*, 221–231. https://doi.org/10.2741/3923
66. Bhattarai, N.; Scott, I. In the heart and beyond: Mitochondrial dysfunction in Heart Failure with preserved Ejection Fraction (HFpEF). *Curr. Opin. Pharmacol*. **2024**, *76*, 102461. https://doi.org/10.1016/j.coph.2024.102461
67. Hasenfuss, G.; Reinecke, H.; Studer, R.; Meyer, M.; Pieske, B.; Holtz, J.; Holubarsch, C.; Posival, H.; Just, H.; Drexler, H. Relation between myocardial function and expression of sarcoplasmic reticulum Ca^{2+}-ATPase in failing and nonfailing human myocardium. *Circ. Res*. **1994**, *75*, 434–442. https://doi.org/10.1161/01.res.75.3.434
68. Eisner, D.; Caldwell, J.; Trafford, A. Sarcoplasmic reticulum Ca-ATPase and heart failure 20 years later. *Circ. Res*. **2013**, *113*, 958–961. https://doi.org/10.1161/CIRCRESAHA.113.302187
69. Mansour, T.E. Phosphofructokinase activity in skeletal muscle extracts following administration of epinephrine. *J. Biol. Chem*. **1972**, *247*, 6059–6066.
70. Su, J.Y.; Storey, K.B. Regulation of phosphofructokinase from muscle and liver of rainbow trout by protein phosphorylation. *Biochem. Mol. Biol. Int*. **1994**, *33*, 1191–1200.
71. Reed, M.C.; Lieb, A.; Nijhout, H.F. The biological significance of substrate inhibition: a mechanism with diverse functions. *Bioessays*. **2010**, *32*, 422–429. https://doi.org/10.1002/bies.200900167
72. Sharov, V.S.; Dremina, E.S.; Galeva, N.A.; Williams, T.D.; Schöneich, C. Quantitative mapping of oxidation-sensitive cysteine residues in SERCA in vivo and in vitro by HPLC-electrospray-tandem MS: selective protein oxidation during biological aging. *Biochem. J*. **2006**, *394*, 605–615. https://doi.org/10.1042/BJ20051214
73. Horáková, L.; Strosova, M.K.; Spickett, C.M.; Blaskovic, D. Impairment of calcium ATPases by high glucose and potential pharmacological protection. *Free Radic. Res*. **2013**, *47*, 81–92. https://doi.org/10.3109/10715762.2013.807923
74. Borlaug, B.A.; Jensen, M.D.; Kitzman, D.W.; Lam, C.S.P.; Obokata, M.; Rider, O.J. Obesity and heart failure with preserved ejection fraction: new insights and pathophysiological targets. *Cardiovasc. Res*. **2023**, *118*, 3434–3450. https://doi.org/10.1093/cvr/cvac120
75. Mouton, A.J.; Li, X.; Hall, M.E.; Hall, J.E. Obesity, hypertension, and cardiac dysfunction: novel roles of immunometabolism in macrophage activation and inflammation. *Circ. Res*. **2020**, *126*, 789–806. https://doi.org/10.1161/CIRCRESAHA.119.312321
76. Paulus, W.J.; Zile, MR. From systemic inflammation to myocardial fibrosis: the heart failure with preserved ejection fraction paradigm revisited. *Circ. Res*. **2021**, *128*, 1451–1467. https://doi.org/10.1161/CIRCRESAHA.121.318159
77. Ndumele, C.E.; Neeland, I.J.; Tuttle, K.R.; Chow, S.L.; Mathew, R.O.; Khan, S.S.; Coresh, J.; Baker-Smith, C.M.; Carnethon, M.R.; Després, J.P.; Ho, J.E.; Joseph, J.J.; Kernan, W.N.; Khera. A.; Kosiborod, M.N.; Lekavich, C.L.; Lewis, E.F.; Lo, K.B.; Ozkan, B.; Palaniappan, L.P.; Patel, S.S.; Pencina, M.J.; Powell-Wiley, T.M.; Sperling, L.S.; Virani, S.S.; Wright, J.T.; Rajgopal Singh, R.; Elkind, M.S.V.; Rangaswami, J.; American Heart Association. A Synopsis of the Evidence for the Science and Clinical Management of Cardiovascular-Kidney-Metabolic (CKM) Syndrome: A Scientific Statement From the American Heart Association. *Circulation*. **2023**, *148*, 1636–1664. https://doi.org/10.1161/CIR.0000000000001186

78. Robotham, J.L.; Takata, M.; Berman, M.; Harasawa, Y. Ejection fraction revisited. *Anesthesiology*. **1991**, *74*, 172–183. https://doi.org/10.1097/00000542-199101000-00026
79. Anand, I.S.; Liu, D.; Chugh, S.S.; Prahash, A.J.; Gupta, S.; John, R.; Popescu, F.; Chandrashekhar, Y. Isolated myocyte contractile function is normal in postinfarct remodeled rat heart with systolic dysfunction. *Circulation*. **1997**, *96*, 3974–3984. https://doi.org/10.1161/01.cir.96.11.3974
80. Kosaraju, A.; Goyal, A.; Grigorova, Y.; Makaryus, A.N. Left Ventricular Ejection Fraction. In: StatPearls [Internet]. Treasure Island (FL): StatPearls Publishing, 2023.
81. Percie du Sert, N.; Hurst, V.; Ahluwalia, A.; Alam, S.; Avey, M.T.; Baker, M.; Browne, W.J.; Clark, A.; Cuthill, I.C.; Dirnagl, U.; Emerson, M.; Garner, P.; Holgate, S.T.; Howells, D.W.; Karp, N.A.; Lazic, S.E.; Lidster, K.; MacCallum, C.J.; Macleod, M.; Pearl, E.J.; Petersen, O.H.; Rawle, F.; Reynolds, P.; Rooney, K.; Sena, E.S.; Silberberg, S.D.; Steckler, T.; Würbel, H. The ARRIVE guidelines 2.0: updated guidelines for reporting animal research. *Br. J. Pharmacol*. **2020**, *177*, 3617–3624. https://doi.org/10.1111/bph.15193
82. Light, K.E.; Kane, C.J.; Pierce, D.R.; Jenkins, D.Ge,Y.; Brown, G.; Yang, H.; Nyamweya, N. Intragastric intubation: important aspects of the model for administration of ethanol to rat pups during the postnatal period. *Alcohol Clin. Exp. Res*. **1998**, *22*, 1600−1606. https://doi.org/10.1111/j.1530-0277.1998.tb03954.x
83. Dickinson, H.; Moss, T.J.; Gatford, K.L.; Moritz, K.M.; Akison, L.; Fullston, T.; Hryciw, D.H.; Maloney, C.A.; Morris, M.J.; Wooldridge, A.L.; Schjenken, J.E.; Robertson, S.A.; Waddell, B.J.; Mark, P.J.; Wyrwoll, C.S.; Ellery, S.J.; Thornburg, K.L.; Muhlhausler, B.S.; Morrison, J.L. A review of fundamental principles for animal models of DOHaD research: an Australian perspective. *J. Dev. Orig. Health Dis*. **2016**, *7*, 449–472. https://doi.org/10.1017/S2040174416000477
84. Dostanic, I.; Schultz Jel, J.; Lorenz, J.N.; Lingrel, J.B. The α1 isoform of Na,K-ATPase regulates cardiac contractility and functionally interacts and co-localizes with the Na/Ca exchanger in heart. *J. Biol. Chem*. **2004**, *279*, 54053–54061. https://doi.org/10.1074/jbc.M410737200
85. Lowry, O.H.; Rosebroug, N.J.; Farr, A.L.; Randall, R.J. Protein measurement with the Folin phenol reagent. *J. Biol. Chem*. **1951**, *193*, 265–275.
86. Laemmli, U.K. Cleavage of structural proteins during the assembly of the head of bacteriophage T4. *Nature*. **1970**, *227*, 680–685. https://doi.org/10.1038/227680a0
87. Taussky, H.H.; Shorr, E. A microcolorimetric method for the determination of inorganic phosphorus. *J. Biol. Chem*. **1953**, *202*, 675–685.
88. Sorenson, M.M.; Coelho, H.S.; Reuben, J.P. Caffeine inhibition of calcium accumulation by the sarcoplasmic reticulum in mammalian skinned fibers. *J. Membr. Biol*. **1986**, *90*, 219–230. https://doi.org/10.1007/BF01870128
89. Lang, R.M.; Bierig, M.; Devereux, R.B.; Flachskampf, F.A.; Foster, E.; Pellikka, P.A.; Picard, M.H.; Roman, M.J.; Seward, J.; Shanewise, J.S.; Solomon, S.D.; Spencer, K.T.; Sutton, M.S.; Stewart, W.J.; Chamber Quantification Writing Group; American Society of Echocardiography's Guidelines and Standards Committee; European Association of Echocardiography. Recommendations for chamber quantification: a report from the American Society of Echocardiography's Guidelines and Standards Committee and the Chamber Quantification Writing Group, developed in conjunction with the European Association of Echocardiography, a branch of the European Society of Cardiology. *J. Am. Soc. Echocardiogr*. **2005**, *18*, 1440–1463. https://doi.org/10.1016/j.echo.2005.10.005